01 Jan 2003

A Novel Dual Heuristic Programming Based Optimal Control of a Series Compensator in the Electric Power Transmission System

Jung-Wook Park

Ganesh K. Venayagamoorthy
Missouri University of Science and Technology

Ronald G. Harley

A Novel Dual Heuristic Programming Based Optimal Control of a Series Compensator in the Electric Power Transmission System

Jung-Wook Park and Ronald G. Harley, *Fellow, IEEE*

School of Electrical and Computer Engineering
Georgia Institute of Technology
GA 30332-0250, U.S.A.
(e-mails: jungwookpark@ieee.org and ron.harley@ece.gatech.edu)

Ganesh K. Venayagamoorthy, *Senior Member, IEEE*

Department of Electrical and Computer Engineering
University of Missouri-Rolla
MO 65409-0249, U.S.A.
(e-mail: gkumar@ieee.org)

Abstract – In this paper, the dual heuristic programming (DHP) optimization algorithm is used for the design of a nonlinear optimal neurocontroller that replaces the proportional-integral (PI) based conventional linear controller (CONVC) in the internal control of a power electronic converter based series compensator in the electric power transmission system. The performance of the proposed DHP based neurocontroller is compared with that of the CONVC with respect to damping low frequency oscillations. Simulation results using the PSCAD/EMTDC software package are presented.

I. Introduction

In the last decade, flexible ac transmission system (FACTS) devices [1]-[4] have been progressively developed for controlling power flow in a power transmission system, improving the transient stability, damping power system oscillations, and providing voltage stability by using high power semiconductor technology based inverters connected to the electric power grid.

Recently, the static synchronous series compensator (SSSC) [5]-[7] among the FACTS device family has attracted considerable attention for damping of low frequency power oscillations in the lines by using controllable series voltage compensation.

The internal control strategy for the inverter of a SSSC as well as other FACTS devices has traditionally been based on linear proportional-integral (PI) regulators. These conventional PI linear controllers (CONVC) operate well at one particular operating point where they have been designed. In other words, their transient and dynamic performances are degraded at any other operating point, or their gains have to be re-tuned for the new operating points.

Artificial neural networks (ANNs) can offer an efficient alternative to overcome the above limitation of the CONVC for the internal control. However, only a few researchers [8], [9] have reported on FACTS device control using ANNs in the literature due to the difficulty of implementing an effective and fast internal control of the inverter with the ANNs.

The recently developed adaptive critic designs (ACDs) [10]-[16] based techniques avoid the possibility of instability of the neurocontroller, and also yield an optimal response [17]-[18].

This paper proposes a novel intelligent internal control approach using the multilayer perceptron neural network (MLPNN) as an optimal nonlinear neurocontroller.

The background of the dual heuristic programming (DHP) algorithm, which has the best robust control capability among the ACDs family, is presented. Based on the DHP algorithm, a novel nonlinear optimal neurocontroller (called DHPNC) is designed as an alternative for internal control of the SSSC, thereby replacing the PI based regulators for the currents but not for the dc link voltage. The performances of the DHPNC and CONVC are compared with respect to the damping of power oscillations by time-domain simulations in the PSCAD/EMTDC software package.

II. Static Synchronous Series Compensator (SSSC)

The static synchronous series compensator (SSSC) converter can control the reactive and/or active power on an ac system by changing both phasor angle and magnitude of the converter's output voltage with a fast control action. Especially, the exchange of active power, which is the particular characteristic of the SSSC, is accomplished by controlling the dc voltage inside the SSSC [1].

A. Modeling of SSSC

The single machine infinite bus (SMIB) system shown in Fig. 1 is used to compare the damping control capabilities of the proposed DHPNC and CONVC for the SSSC. The plant consists of the synchronous generator (160 MVA, 15 kV (L-L)), turbine-governor system, automatic voltage regulator (AVR)-exciter system, transmission line connected to an infinite bus, and the SSSC connected in series with transmission line. The parameters of the synchronous generators and transmission line are given in [19].

The EXAC1A (IEEE alternator supplied rectifier excitation systems) and H_TUR1/GOV1 (IEEE type hydro turbine-governor) models in PSCAD/EMTDC software package [20] are used as the AVR/exciter system and turbine/governor, respectively.

0-7803-7898-9/03/$17.00 ©2003 IEEE

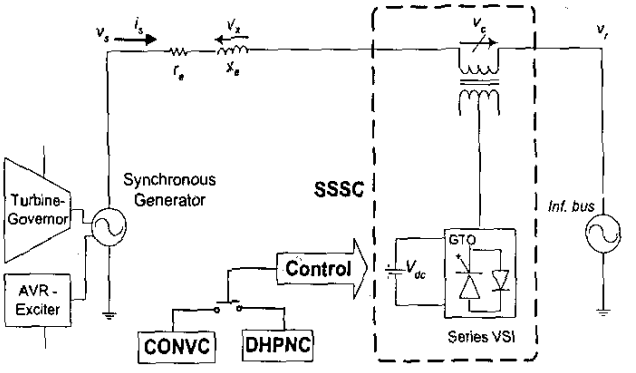

Fig. 1. Plant: 160 MVA, 15 kV (L-L) SMIB test system

For the mathematical model of the SSSC, the associated equation can be represented with the lumped series transmission line reactance x_e' (transmission line x_e plus leakage reactance of series-connected transformer) and transmission series resistance r_e (the inverter is regarded simply to have no conduction losses) in per unit as follows.

$$\frac{d}{dt}\begin{bmatrix} i_{sa} \\ i_{sb} \\ i_{sc} \end{bmatrix} = \begin{bmatrix} -\frac{r_e\omega_s}{x_e'} & 0 & 0 \\ 0 & -\frac{r_e\omega_s}{x_e'} & 0 \\ 0 & 0 & -\frac{r_e\omega_s}{x_e'} \end{bmatrix} \begin{bmatrix} i_{sa} \\ i_{sb} \\ i_{sc} \end{bmatrix} + \begin{bmatrix} \frac{\omega_s}{x_e'}(v_{sa}+v_{ca}-v_{ra}) \\ \frac{\omega_s}{x_e'}(v_{sb}+v_{cb}-v_{rb}) \\ \frac{\omega_s}{x_e'}(v_{sc}+v_{cc}-v_{rc}) \end{bmatrix} \quad (1)$$

where ω_s is the synchronous speed of the power system, v_s is the sending-end voltage (terminal voltage in practice), i_s is the current in transmission line, v_r is the receiving-end voltage in the infinite bus, and v_c is the injected series compensation voltage.

Using the synchronously rotating reference frame based transformation [2], in which the *d-axis is always coincident with the instantaneous voltage vector v and the q-axis leads the d-axis by 90°*, the three-phase circuit equation in (1) can be transformed to the following d-q axis vector representation.

$$\frac{d}{dt}\begin{bmatrix} i_d \\ i_q \end{bmatrix} = \begin{bmatrix} -\frac{r_e\omega_s}{x_e'} & \omega \\ -\omega & -\frac{r_e\omega_s}{x_e'} \end{bmatrix} \begin{bmatrix} i_d \\ i_q \end{bmatrix} + \begin{bmatrix} \frac{\omega_s}{x_e'}(|v_s|+v_{cd}-v_{rd}) \\ \frac{\omega_s}{x_e'}(v_{cq}-v_{rq}) \end{bmatrix} \quad (2)$$

Neglecting the series inverter harmonics, the ac side injected voltage v_c in Fig.1 can be expressed with relation to the capacitor voltage V_{dc} on the dc link as follows.

$$v_{cd} = mV_{dc}\cos(\alpha), \quad v_{cq} = mV_{dc}\sin(\alpha) \quad (3)$$

where α is the phase voltage difference between the voltages v_c and v_s (the v_c leads the v_s), and m is the modulation index of the series inverter. The dynamics of the dc capacitor voltage is given by

$$\frac{dV_{dc}}{dt} = \frac{1}{C}\frac{P_{dc}}{V_{dc}} = \frac{1}{C}\frac{V_{dc}i_{dc}}{V_{dc}} = \frac{1}{C}\frac{(v_{cd}i_d + v_{cq}i_q)}{V_{dc}} \quad (4)$$
$$= \frac{1}{C}\left[m\{\cos(\alpha)i_d + \sin(\alpha)i_q\}\right]$$

B. Conventional Control Strategy

The main goal of the SSSC is to inject the series voltage in quadrature with the line current and to maintain the dc voltage V_{dc}. For this purpose, the *P-Q* (real and reactive power) automatic power flow control mode [1] in Fig. 2 is used.

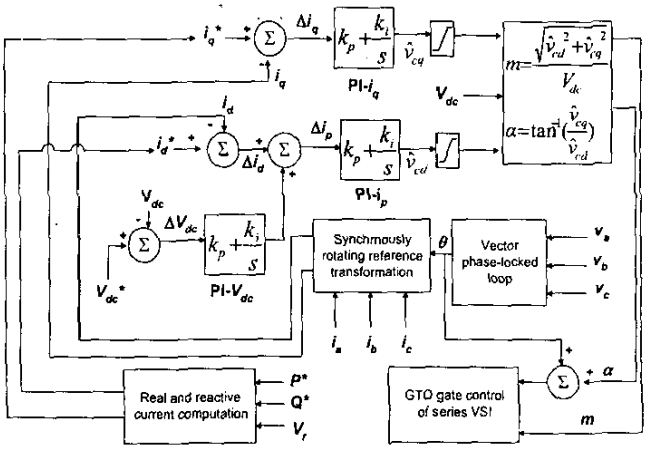

Fig. 2. *P-Q* automatic power flow control diagram for the internal control of the SSSC

In Fig. 2, an instantaneous three-phase set of line voltages, v_a, v_b, and v_c is used to calculate the transformation angle, θ provided by the vector phase-locked loop for synchronous operation of the series voltage source inverter (VSI) shown in Fig.1. As shown in (2), the three-phase set of measured line currents at the ac terminal of the SSSC is decomposed into its real/direct component, i_d, and reactive/quadrature component, i_q. These actual signals (i_d and i_q) and the reference d-q current signals (i_d^* and i_q^*) are compared, respectively.

The error signal Δi_q for the reactive power exchange is passed through the PI regulator PI-i_q. The signal Δi_p for the real power exchange and maintenance of a constant V_{dc}, is passed through the PI-i_p. The Δi_p consists of the Δi_d and error signal ΔV_{dc}, which has been passed through the PI-V_{dc}. The V_{dc}^* is the desired value for V_{dc}.

Finally, the estimated signals ($\hat{v}_{cq}$ and $\hat{v}_{cd}$) in Fig. 2 are used to compute the angle α and modulation index m to drive the gate turn-off (GTO) thyristor of the inverter.

III. DHP Based Neurocontroller Design

Adaptive critic designs (ACDs) proposed by Werbos [11] are new optimization techniques to handle the nonlinear optimal control problem using artificial neural networks.

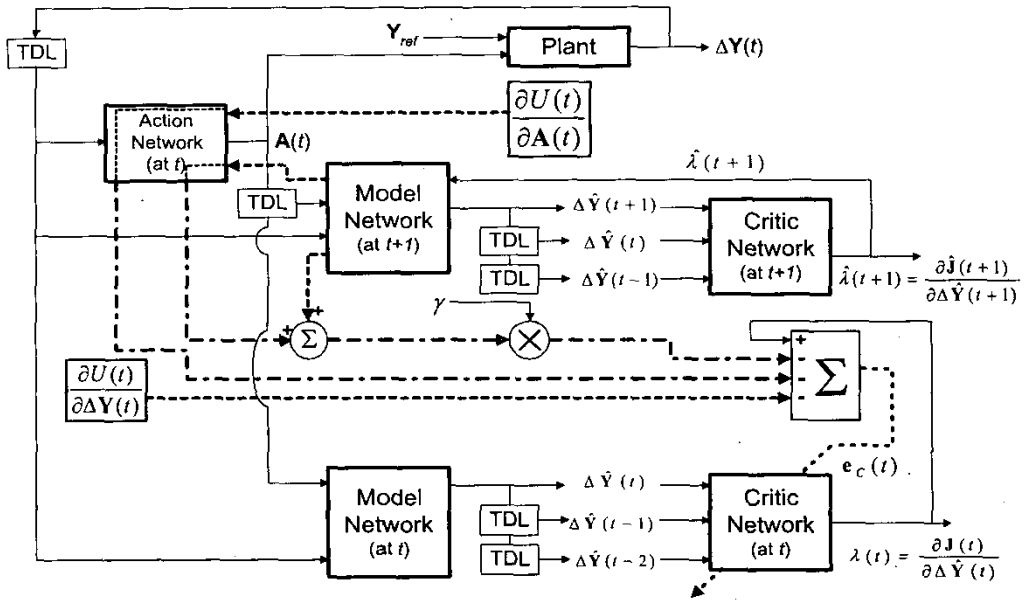

Fig. 3. Critic network adaptation in DHP: This diagram shows the implementation of (8). The same critic network is shown for two consecutive times, t and $t+1$. The discount factor γ is chosen to be 0.5. Backpropagation paths are shown by dotted and dash-dot lines. The output of the critic network $\hat{\lambda}(t+1)$ is backpropagated through the model network from its outputs to its inputs, yielding the first term of (7) and $\partial\mathbf{J}(t+1)/\partial\mathbf{A}(t)$. The latter is backpropagated through the action network from its outputs to its inputs forming the second term of (7). Backpropagation of the vector $\partial U(t)/\partial\mathbf{A}(t)$ through the action network results in a vector with components computed as the last term of (8). The summation of all these signals produces the error vector $\mathbf{e}_c(t)$ used for training the critic network.

The adaptive critic method finds the optimal control in the *infinite horizon problem* to minimize/maximize the user-defined heuristic cost-to-go function **J** for a system, by successively adapting two ANNs, namely the ***action network*** (which dispenses the control signals) and the ***critic network*** (which learns to approximate the cost-to-go function **J**). This process is called the *approximate dynamic programming* (ADP) for the value iteration **J**. The adaptation process starts with a non-optimal, arbitrarily chosen, control by the action network; the critic network then guides the action network towards the optimal solution at each successive adaptation. During the adaptations, neither of the networks needs any 'information' of an optimal trajectory, only the desired cost needs to be known [12]. A more detailed explanation of ACDs technique is given in [10]-[16].

The dual heuristic programming (DHP) technique (among the ACDs family) has the strong control capability in that the critic network of the DHP approximates the derivatives of the function **J** with respect to the states of the plant to be controlled. The DHP algorithm described in this paper uses three different multilayer (three layer) perceptron neural networks (MLPNNs), namely one for each of the critic, model, and action networks.

The weight vector **V** of the MLPNN is adjusted/trained using the gradient descent based backpropagation algorithm. By trial and error, fourteen neurons are used in the hidden layer of the MLPNN for the model network, and ten neurons for each of the critic and action networks.

A. Critic Network

As mentioned before, the DHPNC is designed to replace the PI regulators PI-i_q and PI-i_p in Fig.2. The input reference vector $\mathbf{Y}_{ref}$ into the SSSC and output vector **Y** from the SSSC are:

- $\mathbf{Y}_{ref}(t)$, input reference vector to the SSSC = $[i_p^*(t),\ i_d^*(t),\ V_{dc}^*(t)]$.
- $\Delta\mathbf{Y}(t)$, output vector from the SSSC = $[\,\Delta i_q(t), \Delta i_p(t)\,]$.

The configuration for the critic network adaptation in the DHP is shown in Fig. 3. The inputs and outputs of the action and model networks used in the critic network adaptation are shown in Figs. 4 and 5.

The critic network estimates the derivatives of function **J** with respect to the vector of observables of the plant (identified by the model network), which is the $\Delta\hat{\mathbf{Y}}(t)=[\,\Delta\hat{i}_q(t),\Delta\hat{i}_p(t)\,]$ (input vector of the critic network), and it learns to minimize the following error measure over time:

$$\|E_C\| = \sum_t \mathbf{e}_C^T(t)\mathbf{e}_C(t) \tag{5}$$

$$\mathbf{e}_C(t) = \frac{\partial\mathbf{J}[\Delta\hat{\mathbf{Y}}(t)]}{\partial\Delta\hat{\mathbf{Y}}(t)} - \gamma\frac{\partial\hat{\mathbf{J}}[\Delta\hat{\mathbf{Y}}(t+1)]}{\partial\Delta\mathbf{Y}(t)} - \frac{\partial U[\Delta\mathbf{Y}(t)]}{\partial\Delta\mathbf{Y}(t)} \tag{6}$$

After exploiting all relevant pathways of backpropagation as shown in Fig. 3, where the paths of derivatives and adaptation of the critic network are depicted by dotted and

dash-dot lines, the error signal $\mathbf{e}_C(t)$ is used for training to update the weights of the critic network.

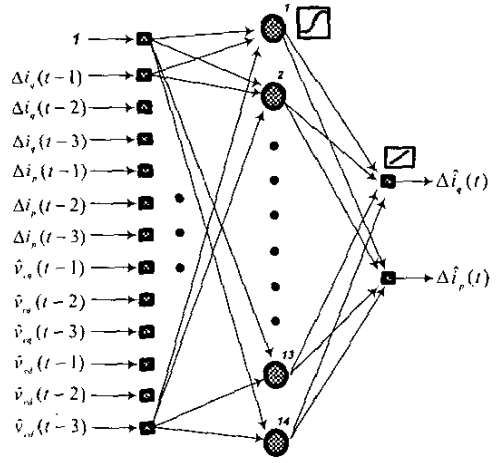

Fig. 4. Input-output mapping of the model network at t used in the critic network adaptation in Fig. 3.

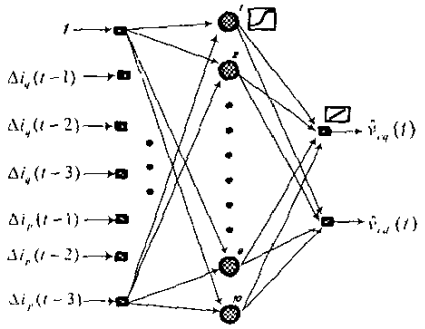

Fig. 5. Input-output mapping of the action network at t used in the critic network adaptation in Fig. 3.

The j^{th} component of the second term in (6) can be expressed by the output of critic network at time $t+1$, $\hat{\lambda}_i(t+1) = \partial \hat{\mathbf{J}}[\Delta \hat{\mathbf{Y}}(t+1)] / \partial \Delta \hat{\mathbf{Y}}_i(t+1)$ as follows.

$$\frac{\partial \hat{\mathbf{J}}[\Delta \hat{\mathbf{Y}}(t+1)]}{\partial \Delta \mathbf{Y}_j(t)} = \sum_{i=1}^{n} \hat{\lambda}_i(t+1) \frac{\partial \hat{\mathbf{Y}}_i(t+1)}{\partial \Delta \mathbf{Y}_j(t)} + \sum_{k=1}^{m} \sum_{i=1}^{n} \hat{\lambda}_i(t+1) \frac{\partial \Delta \hat{\mathbf{Y}}_i(t+1)}{\partial \mathbf{A}_k(t)} \frac{\partial \mathbf{A}_k(t)}{\partial \Delta \mathbf{Y}_j(t)} \tag{7}$$

where n and m are the numbers of outputs of the model and the action networks, respectively. By using (7), each component of the vector $\mathbf{e}_C(t)$ from (6) is determined by

$$\mathbf{e}_{Cj}(t) = \frac{\partial \mathbf{J}[\Delta \hat{\mathbf{Y}}(t)]}{\partial \Delta \hat{\mathbf{Y}}_j(t)} - \gamma \frac{\partial \hat{\mathbf{J}}[\Delta \hat{\mathbf{Y}}(t+1)]}{\partial \Delta \mathbf{Y}_j(t)} - \frac{\partial U[\Delta \mathbf{Y}(t)]}{\partial \Delta \mathbf{Y}_j(t)} - \sum_{k=1}^{m} \frac{\partial U[\Delta \mathbf{Y}(t)]}{\partial \mathbf{A}_k(t)} \frac{\partial \mathbf{A}_k(t)}{\partial \Delta \mathbf{Y}_j(t)} \tag{8}$$

Using (8), the expression for the weights' update for the critic network is as follows.

$$\Delta \mathbf{V}_C(t) = -\eta_C \mathbf{e}_C^{\mathrm{T}}(t) \frac{\partial \mathbf{e}_C(t)}{\partial \mathbf{V}_C(t)} \tag{9}$$

where η_C is a positive learning rate and $\mathbf{V}_C$ contains the weights of the DHP critic network.

B. Action Network

The adaptation of the action network in Fig. 3 is illustrated in Fig. 6, which propagates $\hat{\lambda}(t+1)$ back through the model network to the action network. The goal of this adaptation is expressed in (10), and the weights of the action network are updated by (11). As described before, the output vector of the action network is $\mathbf{A}(t)=[\hat{v}_{cq}(t), \hat{v}_{cd}(t)]$.

$$\frac{\partial U[\Delta \mathbf{Y}(t)]}{\partial \mathbf{A}(t)} + \gamma \frac{\partial \hat{\mathbf{J}}[\Delta \hat{\mathbf{Y}}(t+1)]}{\partial \mathbf{A}(t)} = 0 \quad \forall t. \tag{10}$$

$$\Delta \mathbf{V}_A(t) = -\eta_A [\frac{\partial U[\Delta \mathbf{Y}(t)]}{\partial \mathbf{A}(t)} + \gamma \frac{\partial \hat{\mathbf{J}}[\Delta \hat{\mathbf{Y}}(t+1)]}{\partial \mathbf{A}(t)}]^{\mathrm{T}} \frac{\partial \mathbf{A}(t)}{\partial \mathbf{V}_A(t)} \tag{11}$$

where η_A is a positive learning rate and $\mathbf{V}_A$ contains the weights of the DHP action network.

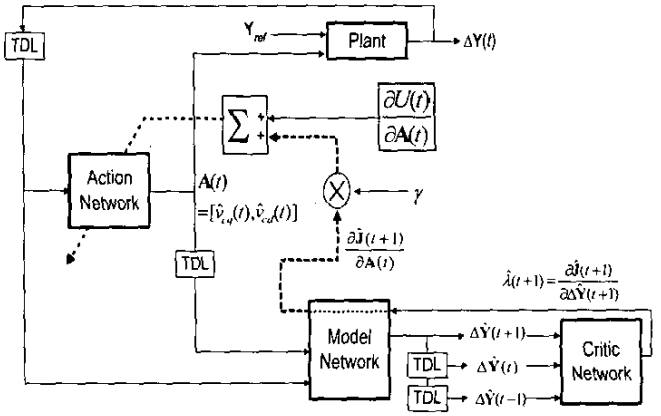

Fig. 6. Action network adaptation in DHP: The discount factor γ is chosen to be 0.5. Backpropagation paths are shown by dotted lines. The output of the critic network $\hat{\lambda}(t+1)$ at time $(t+1)$ is backpropagated through the model network from its outputs to its inputs (output of the action network), and the resulting vector multiplied by the discount factor (γ = 0.5) and added to $\partial U(t)/\partial \mathbf{A}(t)$. Then, an incremental adaptation of the action network is carried out by (10) and (11)

The discount factor γ of 0.5 and the user-defined utility function $U(t)$ [10] in (12) are used in (8) and (10) during adaptation of the critic and action networks.

$$U(t) = \left[\Delta i_q(t) + \Delta i_q(t-1) + \Delta i_q(t-2)\right]^2 + \left[\Delta i_p(t) + \Delta i_p(t-1) + \Delta i_p(t-2)\right]^2 \tag{12}$$

C. Model Network

Fig. 7 illustrates how the model network (identifier) is trained to identify the dynamics of the plant in Fig. 1. The nonlinear autoregressive moving average with exogenous

inputs (NARMAX) model is used as the structure for the on-line identification. The components of vectors $\mathbf{Y}_{ref}(t)$, $\Delta\mathbf{Y}(t)$, $\mathbf{A}(t)$, and $\Delta\hat{\mathbf{Y}}(t)$ are already noted in section *A* above (see Figs. 4 and 5). The residual vector, $\mathbf{e}_M(t)$ given in (13) is used for updating the model network's weights $\mathbf{V}_M$ in (14) during training by the backpropagation algorithm.

$$\mathbf{e}_M(t) = \Delta\mathbf{Y}(t) - \Delta\hat{\mathbf{Y}}(t) = [\Delta i_q(t) - \Delta\hat{i}_q(t),\ \Delta i_p(t) - \Delta\hat{i}_p(t)] \quad (13)$$

$$\Delta\mathbf{V}_M(t) = -\eta_M \mathbf{e}_M^{\mathrm{T}}(t)\frac{\partial \mathbf{e}_M(t)}{\partial \mathbf{V}_M(t)} \quad (14)$$

where η_M is a positive learning rate and $\mathbf{V}_M$ is the weights of the DHP model network.

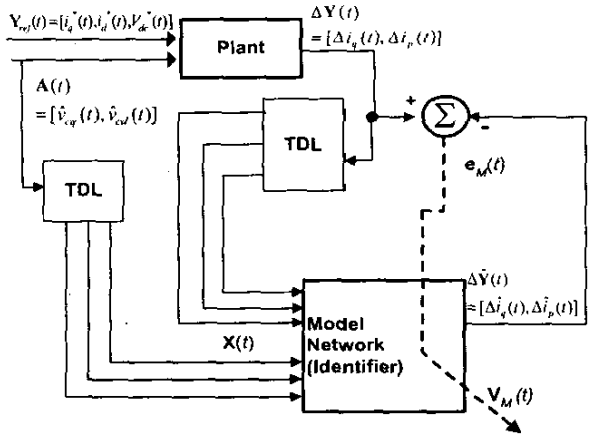

Fig. 7. NARMAX model for on-line training of the model network

The training procedures of the critic, action, and model networks used in the DHP algorithm are explained in [10] and [15]. Note that the model network is trained before the training of the action and critic networks, and the DHPNC with the fixed (converged) weights for the critic and action networks is used to control the plant for real-time operation. In other words, they have been successfully trained to their optimization purposes (value iteration for the critic network and policy iteration for the action network [18]).

IV. Simulation Results

To evaluate the damping performance of the proposed neurocontroller for the control of the SSSC, 100 ms and 120 ms three phase short circuits are applied to the infinite bus at t=1 s. The generator operates with a rotor angle of 53.6° (P_t=1.0 pu, Q_t= 0.59 pu) in a steady-state operating point. The results are shown in Figs. 8 to 12, where "Uncompensated" and "CONVC" denote the response of generator controlled without SSSC and with the PI based SSSC, respectively.

From Fig. 8, it can be observed that the transmission line current i_s leads the compensating injection voltage v_c by almost 90° (considering the r_e) in steady-state such that the SSSC controlled by both the CONVC and DHPNC can establish the same effect as the series capacitive compensation resulting in increasing the line current (i_s) and transmitted power (P). From the Figs. 9 to 10, the DHPNC damping control is more effective compared to the CONVC. Also, it is clear from Figs. 11 and 12 that the generator controlled without the SSSC goes unstable and loses synchronism when the fault duration is 120 ms. In contrast, the DHPNC and CONVC restore the generator to a stable mode, and the DHPNC damping control is more effective compared to the CONVC, which means that the DHPNC allows the generator to be operated closer to its stability limit during steady state by providing sufficient margins of safety.

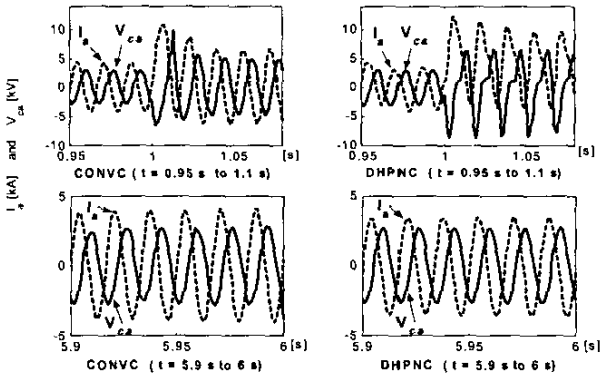

Fig. 8. A 100 ms three phase short circuit test: line current i_a [kA] and injected voltage v_{ca} [kV]

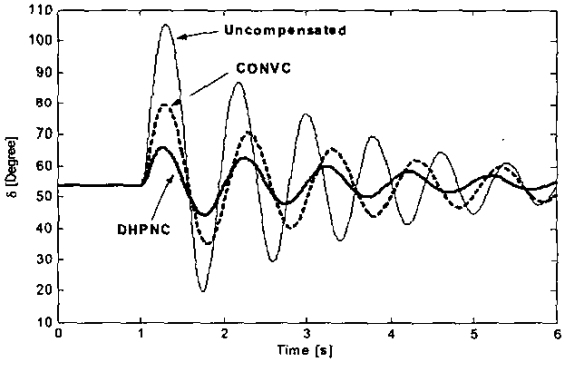

Fig. 9. A 100 ms three phase short circuit test: δ [°]

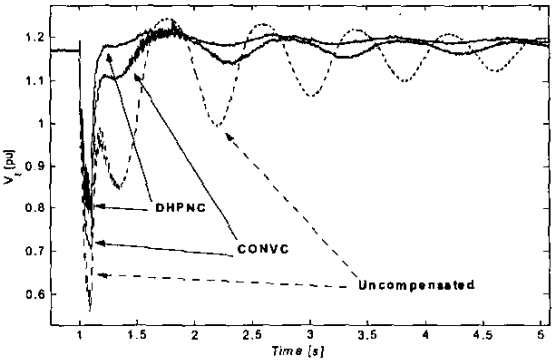

Fig. 10. A 100 ms three phase short circuit test: V_t [pu]

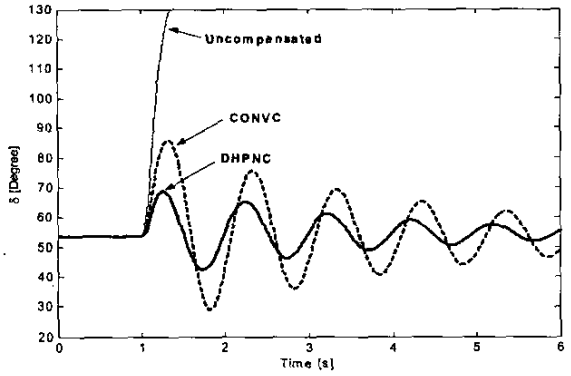

Fig. 11. A 120 ms three phase short circuit test: δ [°]

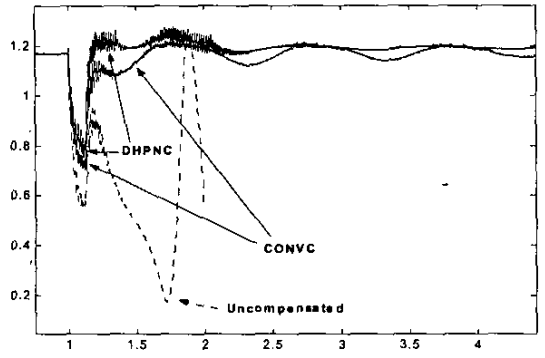

Fig. 12. A 120 ms three phase short circuit test: V_t [pu]

Similar results are obtained for different system disturbances such as a single line-to-ground fault at the generator terminal and multiple short circuits in different points, where are infinite bus and machine terminal.

V. Conclusions

This paper has proposed a novel dual heuristic programming (DHP) based design of a nonlinear optimal neurocontroller (DHPNC) for the internal control of a static synchronous series compensator (SSSC) used in a transmission line of an electric power grid. The multilayer perceptron neural network (MLPNN) is used as function approximator for the critic, action, and model networks to implement the DHP algorithm.

The PSCAD/EMTDC simulation results show that the DHPNC has a better performance than the PI based conventional controller (CONVC) with respect to damping low frequency power oscillations.

The use of fixed parameters in the DHPNC for real-time control not only have an important significance in terms of reducing the number of computations in dealing with the infinite optimal control problem by using the artificial neural networks, but also proves robustness to the adaptive critic designs (ACDs) based controllers.

Acknowledgment

Financial support by the National Science Foundation (NSF), USA under Grant No. ECS-0080764 for this research is gratefully acknowledged.

VI. References

[1] N.G. Hingorani and L. Gyugyi, "Understanding FACTS-Concepts and Technology of Flexible AC Transmission Systems," IEEE Press, New York, 2000, ISBN 0-7803-3455-8.

[2] T. Makombe and N. Jenkins, "Investigation of a unified power flow controller," *IEE Proc.-Gener. Transm. Distrib.*, Vol.146, No.4, pp. 400-408, July 1999.

[3] Schauder, C.D., et al., "Operation of the Unified Power Flow Controller (UPFC) Under Practical Constraints," *IEEE Trans. on Power Delivery*, Vol.13, No.2, pp. 630-639, April 1998.

[4] M. Noroozian, L. Ängquist, M. Ghandhari, G. Andersson, "Improving Power System Dynamics by Series-Connected FACTS Devices," *IEEE Trans. on Power Delivery*, Vol.12, No.4, pp. 1635-1641, October 1997.

[5] Gyugyi, L., et al., "Static Synchronous Series Compensator: A Solid-State Approach to the Series Compensation of Transmission Lines," *IEEE Trans. on Power Delivery*, Vol.12, No.1, pp. 406-417, January 1997.

[6] Kalyan K. Sen, "SSSC-Static Synchronous Series Compensator: Theory, Modeling, and Application," *IEEE Trans. on Power Delivery*, Vol.13, No.1, pp. 241-246, January 1998.

[7] Bruce S. Rigby and R.G. Harley, "An Improved control Scheme for a Series-Capacitive Reactance Compensator Based on a Voltage-Source Inverter," *IEEE Trans. on Industry Applications*, Vol.34, No.2, pp. 355-363, March/April 1998.

[8] M. Mohaddes, A.M. Gole, and P.G. McLaren, "A Neural Network Controlled Optimal Pulse-Width Modulated STATCOM," *IEEE Trans. on Power Delivery*, Vol.14, No.2, pp. 481-488, April 1999.

[9] P. K. Dash, S. Mishra, and G. Panda, "A Radial basis function neural network controller for UPFC," *IEEE Trans. on Power Systems*, Vol.15, No.4, pp. 1293-1299, November 2000.

[10] Jung-Wook Park, R.G. Harley, and G.K. Venayagamoorthy, "Adaptive Critic Based Optimal Neurocontrol for Synchronous Generator in Power System Using MLP/RBF Neural Networks," *37th IEEE Annual Industry Application Society (IAS) Meeting*, Vol. 2, pp.1447-1454, October 2002.

[11] P. J. Werbos, "Approximate dynamic programming for real-time control and neural modeling," in *Handbook of Intelligent Control*, D. White and D. Sofge, Eds. New York: Van Nostrand Reinhold, pp.493-526, 1992.

[12] D.V. Prokhorov, and D.C. Wunsch, "Adaptive critic designs," *IEEE Trans. on Neural Networks*, Vol.8, No.5, pp. 997-1007, Sept. 1997.

[13] D.V. Prokhorov, "Adaptive critic designs and their applications," PhD dissertation, Texas Tech University, USA, 1997.

[14] Jennie Si and Yu-Tsung Wang, "On-Line Learning Control by Association and Reinforcement," *IEEE Trans. on Neural Networks*, Vol.12, No.2, pp. 264-276, March. 2001.

[15] G.K. Venayagamoorthy, R.G. Harley, and D.C. Wunsch, "Comparison of Heuristic Dynamic Programming and Dual Heuristic Programming Adaptive Critics for Neurocontrol of a Turbogenerator," *IEEE Trans. on Neural Networks*, Vol.13, No.3, pp. 764-773, May. 2002.

[16] ——, "Dual heuristic programming excitation neurocontrol for generators in a multimachine power system," to *appear in IEEE Trans. on Industry Applications*, March/April. 2003.

[17] David A. White and Michael I. Jordan, "Optimal control: A foundation for intelligent control," in *Handbook of Intelligent Control*, D. White and D. Sofge, Eds. New York: Van Nostrand Reinhold, pp.185-214, 1992.

[18] Dimitri P. Bertsekas, "Dynamic Programming and Optimal Control", Athena Scientific, Belmont, Massachusetts, 2001.

[19] P.M. Anderson and A.A. Fouad, "Power system control and stability," IEEE Press, New York, 1994, ISBN 0-7803-1029-2.

[20] Manitoba HVDC Research Centre Inc: "Introduction to PSCAD/EMTDC Version 3.0".